Differences between bouncing balls, springs, and rods

Rod Cross[a)]
Physics Department, University of Sydney, Sydney NSW 2006, Australia

(Received 15 January 2008; accepted 30 May 2008)

When one hard steel ball collides with another, kinetic energy is conserved, even if the balls have different diameters. Why is kinetic energy conserved in such a collision, given that kinetic energy is not conserved when two unequal length steel springs or rods collide? Experimental results with bouncing balls, springs, and rods are presented, which reveal the answer. For colliding springs and rods a significant fraction of the initial kinetic energy is retained after the collision as vibrational energy in the longer spring and rod. When two hard balls collide, a negligible fraction of the initial energy is converted to vibrational energy because the collision time is much longer than the transit time of an acoustic wave across each ball due to the fact that the contact region of a hard spherical ball is much softer than the rest of the ball. © *2008 American Association of Physics Teachers.*
[DOI: 10.1119/1.2948778]

I. INTRODUCTION

If a compression spring is dropped onto a floor so that it impacts vertically on one end, the spring bounces off the floor in a manner that appears to be similar to that of a spherical ball. The only difference to the eye is that a spring tends to twist and turn after it bounces because it is difficult to align the spring so that the normal reaction force passes through its center of mass. However, there is a surprising difference in the nature of the force exerted on the floor. When a ball bounces, the force increases to a maximum and then decreases to zero in a way that can be described approximately by the first half cycle of a sinusoidal waveform. The force waveform might be slightly bell shaped and might be slightly asymmetrical, depending on the type of ball, but the force rises to a maximum value when the compression of the ball is near its maximum value. These results indicate that a bouncing ball behaves like a rigid mass attached to the top end of a massless and slightly nonlinear spring. When a compression spring bounces, the force rises rapidly to a certain value, remains constant at that value for a relatively long time, and then drops rapidly to zero as the spring loses contact with the floor. The bottom end of a spring therefore remains compressed by a fixed amount throughout most of the bounce.

The dynamic properties of springs have been investigated in considerable detail,[1–4] although little information on the force acting on a bouncing spring seems to be available. There is a close analogy between springs and rods,[5–9] because both support compressional waves that propagate at speed $v=\sqrt{E/\rho}=L\sqrt{k/m}$, where E is Young's modulus, ρ is the mass density, L is the length, k is the stiffness, and m is the mass of the spring or rod. The duration of an end-on collision between two springs or two long rods is determined by the time taken for a compression wave to propagate from one end of the longer spring or rod to the other and then back again.[4,6] The duration of the bounce of a spring or a long rod dropped onto a heavy, rigid surface is also determined by the round trip propagation time. When a short rod or a ball is dropped onto the surface, the impact duration can be much longer than the transit time of a compression wave along the rod or across the ball, typically by a factor of 10 or more for a steel ball.

A coil spring has its mass and stiffness distributed uniformly along its length. A spherical ball has a different distribution of mass and stiffness along the bounce axis. Why does this distribution have such a strong influence on the behavior of the ball? To investigate the differences several experiments were undertaken to compare the bounce properties of springs and rods with those of a solid ball, and the results were modeled by treating each system as a mass-spring chain.[10,11] The model was used to investigate head-on collisions between two springs and between two elastic balls. It is known that kinetic energy is not conserved when the two springs are of unequal length.[4,6] It is therefore surprising that kinetic energy is almost conserved when the two balls have different diameters. It is shown that both results are consistent with a mass-spring chain model, provided that appropriate mass and stiffness distributions are used to model each system.

II. BOUNCING SPRING EXPERIMENT

The impact force acting on two compression springs was measured by dropping them from a height of 50 cm onto a 50-mm-diam, 8-mm-thick, ceramic piezoelectric disk. The disk was mounted centrally on the end face of an 8.3 kg copper cylinder. The output voltage from a piezo disk is linearly proportional to the force on the disk. An external 20 nF capacitor connected in parallel with the disk was used to extend the time constant to 200 ms when the output voltage was measured with a 10 MΩ resistance voltage probe. The voltage signal was recorded with a 1 MHz bandwidth digital storage oscilloscope. A constant force applied to a piezo disk generates a charge that decays exponentially with time when it is measured with a voltage probe. An accurate force measurement is possible only when the force is applied for a time much less than the time constant, although a correction can be made to take the discharge time constant into account.

Spring A had mass $m=0.145$ kg, length $L=0.18$ m, and stiffness $k=9100$ N/m. It was constructed as a 19 turn coil using 3.4-mm-diam steel wire. Spring B had mass of 0.0618 kg, length 0.30 m, and a stiffness of 30.1 N/m. Spring B was constructed as a 39 turn coil using 1.2-mm-diam steel wire. The impact duration of spring A was 8.0 ms, and the impact duration of spring B was 90 ms, consistent with the fact that the compressional wave speed $L\sqrt{k/m}$ was 44.8 m/s for spring A and 6.6 m/s for spring B. The long duration of the impact for spring B made it possible

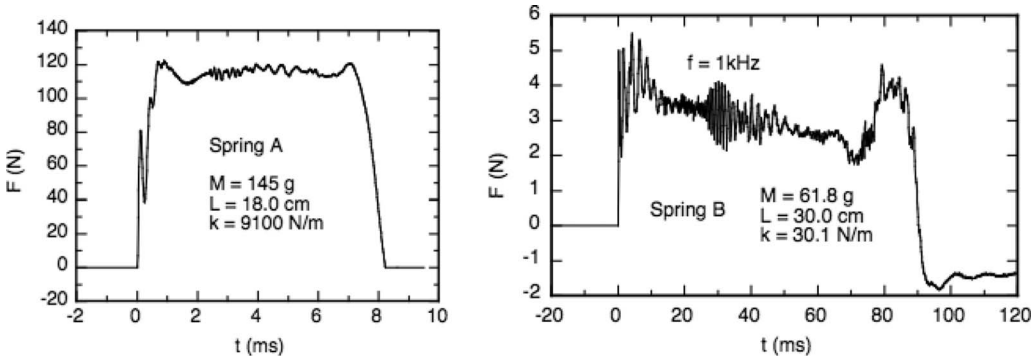

Fig. 1. Force waveforms observed by dropping two springs from a height of 50 cm onto a piezo disk. Spring B wobbled slightly as it bounced, giving a noisier force waveform.

to observe the compression of the spring by filming a bounce with a video camera. A camera operating at 25 or 30 frames/s would have sufficed, but a 100 frames/s camera was used and several identical bounces were filmed to capture the bounce at intervals less than 10 ms apart.

The observed force waveforms for the two springs are shown in Fig. 1. Both force waveforms show evidence of small amplitude, dispersive transverse waves propagating along each spring. This evidence can be seen in the form of small amplitude, high frequency components in the force waveforms, extending up to about 1 kHz. This effect was not investigated in detail but the result is presumably due to transient bending or buckling events occurring during the compression of each spring. The main interest is that the force on each spring remains essentially constant in time, although there is a peak in the force, for both springs A and B, at the beginning and end of the bounce. The measured force waveform for spring B decreased in time, with a time constant of about 200 ms, and then reversed sign at the end of the impact period. Both effects are spurious, resulting from the 200 ms discharge time constant of the measuring circuit. The observed result is consistent with the compression force on the spring remaining essentially constant in time and then decreasing to zero at the end of the impact period. An analogous result would be obtained if a square wave signal were applied to a series *RC* circuit with a time constant of 200 ms and the voltage were measured across the resistor.

The qualitative behavior of spring B as observed on the video is indicated in Fig. 2. The behavior of a spring as it falls through the air is also of interest and has been described previously.[1,2] When the top end of a long spring is released, the bottom end of the spring does not move until the compression wave generated at the top arrives at the bottom. It might be expected that the bottom end would start to fall as soon as the top end is released. A similar effect, in reverse, occurs when the spring bounces off the floor. The bottom end compresses while the top end continues to fall at its initial incident speed. Meanwhile, a compression wave travels up the spring, bringing successive turns of the spring to rest until the entire spring comes to rest. The compression wave then reflects off the top end causing the top end to expand. As the expansion wave travels back down the spring, successive turns expand until the whole spring bounces off the floor.

Each spring was incident at speed $v=3.13$ m/s and came to rest after one transit time, T. Because the momentum decreased to zero at an approximately uniform rate, the force on spring A can be estimated as $mv/T=113.5$ N, and the force on spring B as 4.3 N, in reasonably good agreement with the observed results.

III. BOUNCING BALL EXPERIMENTS

When a steel ball bounces off a steel anvil or collides with another steel ball, the collision time is typically much longer than the time for a pressure wave to propagate across the ball. For example, the impact duration of two 38-mm-diam steel balls colliding at 1 m/s is about 115 μs.[12] The speed of sound in steel is 5100 m/s. Hence, a compressional wave would take only 14.9 μs to travel across two ball diameters, and travels about 15 times across each ball during the impact. Steel balls and steel springs therefore bounce in a very different manner.

To compare the bounce of a ball with the bounce of a spring, several measurements were made using a solid synthetic rubber ball. The ball had a diameter of 60 mm and a mass $m=0.074$ kg. The ball was dropped onto the piezo disk from a height of 50 cm. The result is shown in Fig. 3. The output signal from the piezo was calibrated from the observed change in the velocity of the ball, using the relation $\int F dt = m(v_1+v_2)$, where v_1 is the incident speed and v_2 is the rebound speed. The ball has a coefficient of restitution $v_2/v_1=0.83\pm0.01$. The result shown in Fig. 3 is typical of all spherical balls in that the force waveform can be represented approximately by the first half cycle of a sinusoidal

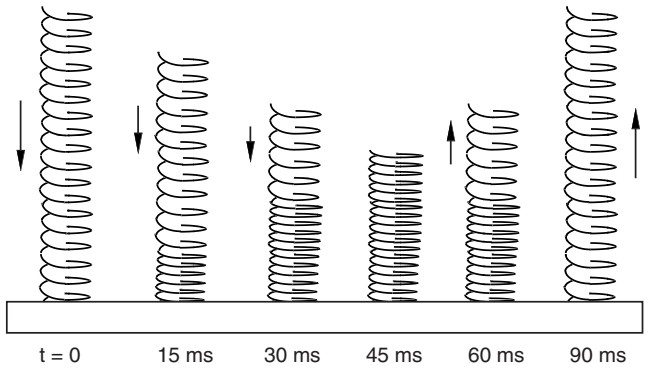

Fig. 2. Behavior of spring B as observed by capturing several identical bounces at 100 frames/s in order to show the spring compression at 15 ms intervals.

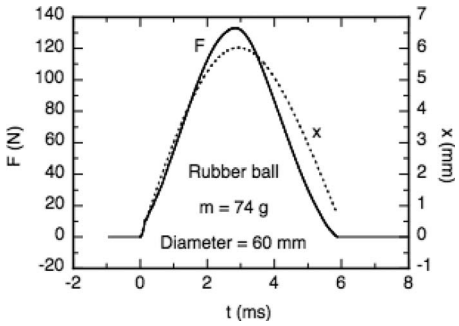

Fig. 3. The force F on a rubber ball and the displacement x of its center of mass when dropped from a height of 50 cm.

waveform.[13] The ball compression was not measured, but the force waveform can be integrated twice to calculate the displacement of the ball center of mass. The result is also shown in Fig. 3, indicating that the ball bounced while it was still slightly compressed.

To analyze the behavior of the ball, estimates were made of its mass and stiffness distributions along the bounce axis. The mass distribution of a solid spherical ball is easily calculated, but the stiffness distribution is difficult to calculate and was measured instead. An identical rubber ball was cut into five parallel slices, each 12 mm thick, and the stiffness of each slice (defined as the load force divided by the compression measured in a direction perpendicular to the flat surfaces) was measured in a materials testing machine. The five slices are labeled as shown in Fig. 4. The mass of each slice is given by $m_1=m_5=0.104M$, $m_2=m_4=0.248M$ and $m_3=0.296M$, where M is the total ball mass.

The force versus compression curves for the top three slices are shown in Fig. 5. The end slices were much softer than the other slices because the cross-sectional area reduces to zero on one side of each slice. If each slice were a cylindrical disk of area A and thickness b, then its stiffness would be given by $k=EA/b$. In theory the stiffness of each end slice is zero when the compression is zero because the contact area would be zero. Small compressions of the end slice can be described by the relation $F=kx^{3/2}$, where x is the compression,[14] in which case the stiffness F/x of the slice is proportional to $x^{1/2}$. However, the stiffness increases more rapidly with x for large compressions. For example, if a thin cylindrical disk is compressed in half, and if the area doubles to maintain the same volume (rubber being incompressible), then the stiffness would increase by a factor of 4. Each disk was compressed by about 4 mm and its stiffness increased by a factor of about 2 or 3 depending on the slice.

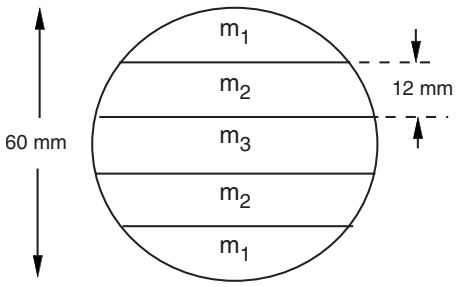

Fig. 4. Five equal thickness segments cut from the rubber ball. The center slice is about three times heavier and stiffer than the end slices.

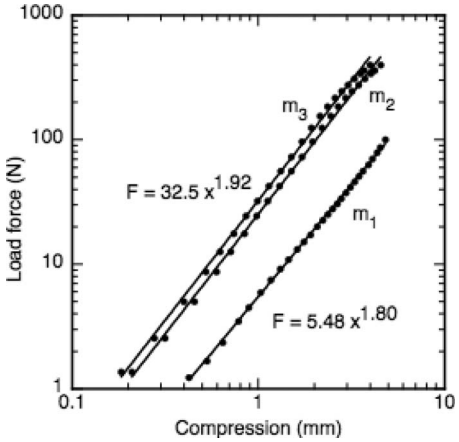

Fig. 5. The measured load force versus the compression x for three of the ball slices, as labeled in Fig. 4. The dots are data points and the straight lines are best fit power laws.

Unlike a simple spring, the stiffness of a rubber (or a steel) ball is a nonlinear function of its compression. The nonlinearity results in a decrease in the impact duration as the incident ball speed increases, because the ball becomes stiffer as its compression increases. The stiffness results in a slightly bell-shaped impact force waveform, but its form has no special significance in terms of the qualitative behavior of the ball. For a 4 mm compression the average stiffness of the central slice was 10% larger than the adjacent slices and three times larger than the end slices.

The stiffness ratio of each element depends on the total compression of the ball. For a very small compression, the contact area of the end slice (of mass m_5) might be less than 1 mm^2, while the end slice and its neighbor maintain contact over a much larger area. At low ball speeds the impact duration of a ball will therefore be extended as a result of the relative softness of the end slice, in which case the compressional wave generated in the ball can make many transits across a ball diameter during the impact. The latter situation arises in a low speed bounce of a steel ball. As will be shown, the rubber ball bounced after about three such transits under the conditions shown in Fig. 3. At lower incident speeds, the rubber ball bounced after several more transits of the compression wave across the ball.

IV. BOUNCING ROD EXPERIMENTS

Aluminum rods of diameter 6.0 and 20.0 mm and various lengths were dropped end-on onto the piezo disk from a height of about 1 cm to measure the impact duration and force waveforms. The bottom end of each rod was rounded with a radius of half the rod diameter to ensure that the rod bounced centrally rather than on an edge and to provide a valid comparison between the different rods. The impact duration is sensitive to the shape and stiffness of the impact end. For example, when the bottom end of a short rod was tapered to a sharp point, the impact duration increased by a factor of about 3, and the impact force decreased by a similar factor, due to the relative softness of the point under compression. Repeated impacts on the pointed end reduced the impact duration and increased the impact force due to the flattening of the initially sharp point. This fact alone shows that the impact force and impact duration of a short rod and

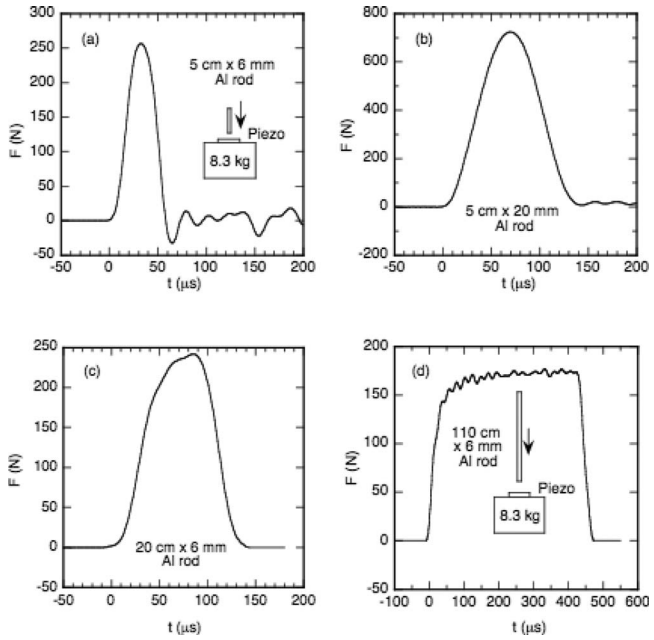

Fig. 6. Force waveforms observed when four aluminum rods were dropped onto the piezo disk, showing the transition from ball-like to spring-like behavior as the rod length increases.

a ball is determined primarily by the stiffness of the contact region rather than by the stiffness of the rod or the ball as a whole. At least, that is the case for a low speed impact. In a high speed impact, a ball might squash in half, in which case the contact region could extend to the center of the ball or beyond.

Results for four such rods are shown in Fig. 6. The 5-cm-long, 6-mm-diam rod had an impact duration of about 50 μs and excited a small amplitude, high frequency vibration of the piezo disk after the impact. The speed of sound in aluminum is 5100 m/s, the same as in steel. During the 50 μs impact there was sufficient time for a compressional wave to make five transits up and down the rod. In that respect short rods bounce in a manner similar to a ball. The normal reaction force varies sinusoidally for one half cycle, as it does during the bounce of a ball. The 5-cm-long, 20-mm-diam rod bounced in a similar manner, but the impact duration was longer than that for the 6-mm-diam rod, despite the fact that the transit time for a compressional wave along each rod was the same. The force waveform for the 20-mm-diam rod was almost identical to that observed for a 30-mm-diam steel ball with the same 130 μs impact duration. The impact duration of the steel ball on the ceramic piezo was slightly longer than that on a steel plate because the ceramic was slightly softer.

The longest 6-mm-diam rod was 1.1 m. Its impact duration was 460 μs, slightly longer than the 431 μs transit time for a compressional wave to propagate up the rod and to reflect back to the bottom end. The normal reaction force for this rod remained approximately constant for most of the bounce period, as it did for a spring. The force waveform for the 20-cm-long rod began to plateau after about 80 μs, but dropped quickly to zero on arrival of the expansion wave reflected from the top end.

The rod results shown in Fig. 6 are similar to those obtained in Ref. 5 using steel rods, and show the changing behavior with rod length and diameter and the relevance to

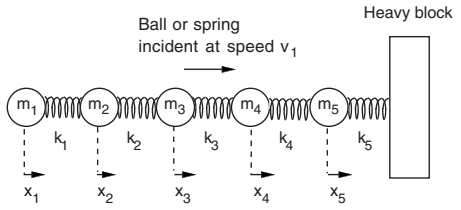

Fig. 7. A chain of five masses and springs incident on a heavy block.

bouncing balls and springs more clearly. The analysis and discussion in Ref. 5 remains relevant, especially that concerning the rise time of the initial compression and the fast fall time at the end of the impact. An alternative analysis is presented in Sec. V based on the mass-spring chain model commonly used to explain the behavior of a crystal lattice and to describe the behavior of Newton's cradle.[8,9,15,16]

Another experiment was undertaken by dropping a 1.2-m-long, 12-mm-diam, 96 g wood dowel onto the piezo. The force waveform was similar to that in Fig. 6(d), and the impact duration was 650 μs, indicating that the speed of sound in the dowel was about 3000 m/s; the first 150 μs and the last 100 μs of the force waveform corresponds to the rise and fall times of the pressure wave in the rod. The purpose of this experiment was to examine the effect of adding a soft, cylindrical rubber tip to the impact end of the rod. The tip was cut from a standard pencil eraser, was 12 mm in diameter, 5 mm thick, and had a mass of 1.6 g. The result was an increase in the impact duration by a factor of about 5, to 3.3 ms, the force waveform being a half cycle sinusoid. We conclude that a long rod bounces like a spring, the impact duration depending primarily on the speed of sound in the rod, and a long rod with a soft tip bounces like a ball with the impact duration depending on the stiffness of the tip and the mass of the rod.

V. BOUNCE MODEL

The bounce of a ball or a spring or rod can be modeled using a discrete chain of masses and springs. The accuracy of the model improves with the number of elements in the chain. A chain of five masses and five springs was used for the calculations presented in the following, corresponding to the number of elements of the ball whose properties were measured. The chain model is shown in Fig. 7. The gravitational force plays only a minor role during the bounce process and is not included in the calculations. The chain is incident in the x direction at speed v_1 when it impacts on a heavy, rigid block. The mass of each element is denoted by m_i, and x_i represents the change in its x coordinate after the chain first makes contact with the block. The equation of motion for each element has the form

$$m_i \frac{d^2 x_i}{dt^2} = F_L - F_R, \tag{1}$$

where F_L is the force in the positive x direction arising from the compression $x_{i-1} - x_i$ of the spring to the left of the mass and F_R is the force in the negative x direction arising from the compression $x_i - x_{i+1}$ of the spring to the right of the mass. The force acting on the block is given by $k_5 x_5$ for a spring obeying Hooke's law.

For a uniform spring or rod of mass m and stiffness k, the mass of each element in the chain can be taken as $m_i = m/5$,

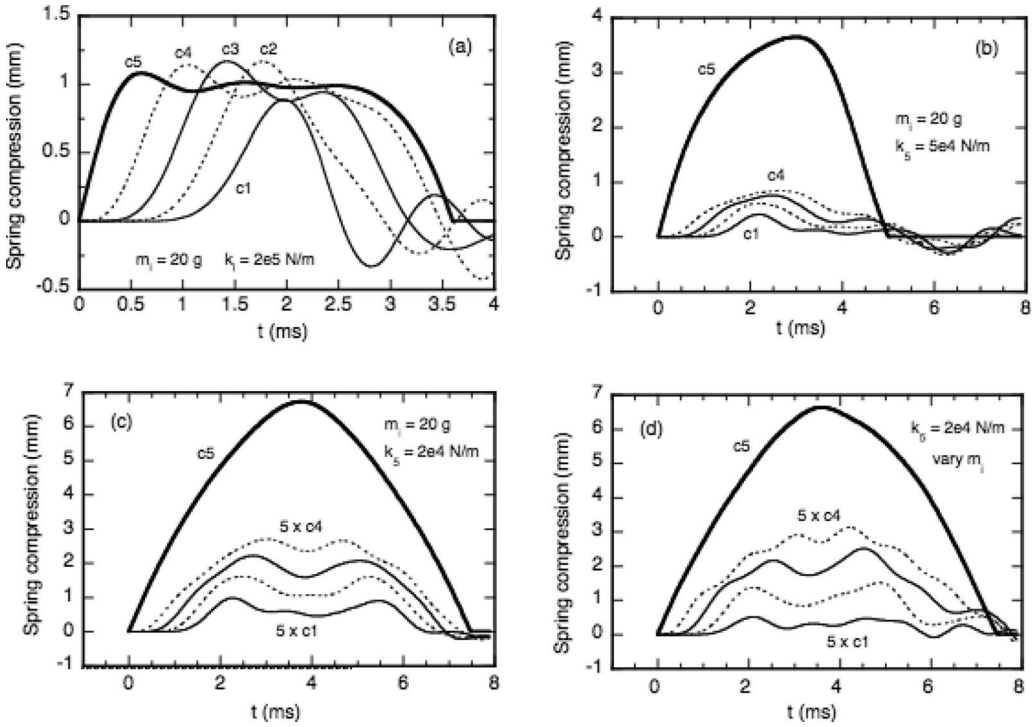

Fig. 8. Numerical solutions of Eq. (1) for four mass-spring chains incident at 3.13 m/s on a rigid surface, showing the compression of each of the five springs in the chain, denoted by c_1–c_5. The impact force waveform is the same as the c_5 waveform, because $F=k_5c_5$. The compression values c_1c_4 are all magnified by a factor of 5 in (c) and (d).

the stiffness of each element can be taken as $k_i=5k$, and the force law for each element is given by Hooke's law. The results described in Sec. III for a spherical ball were used to determine the mass and stiffness of each element. Each experimental result presented in this paper was modeled by a separate chain model, giving good fits to the force waveforms. We present in Fig. 8 a different set of solutions to show the effects of varying the mass and stiffness of the five chain elements in a more systematic manner. Figure 8 shows the results for four mass and stiffness distributions. In each case the compression of each element in the chain is shown as a function of time, assuming that the chain was dropped from a height of 50 cm and impacted a rigid surface at a speed of 3.13 m/s.

Each of the results in Fig. 8 was calculated for a chain of mass $m=0.1$ kg. In Figs. 8(a)–8(c) the mass of each element was the same (0.02 kg); in Fig. 8(d) the mass distribution was taken to be that of a sphere, with $m_1=m_5=0.0104$ kg, $m_2=m_4=0.0248$ kg, and $m_3=0.0296$ kg. In Fig. 8(a) the stiffness of each element was the same with $k_i=2\times10^5$ N/m. The result in Fig. 8(a) is therefore representative of a uniform spring or a long rod. In Fig. 8(b) the element in contact with the rigid surface was taken to be four times softer than the other elements, with $k_5=5\times10^4$ N/m; the other four elements had the same stiffness as in Fig. 8(a). The result in Fig. 8(b) is representative of a medium length rod because the rise time of the pressure disturbance in the rod is about equal to the transit time of the compressional wave along the rod. The only change of the chain shown in Fig. 8(c) compared to Fig. 8(b) is a further reduction in the stiffness of the contact element to $k_5=2\times10^4$ N/m. The result in Fig. 8(c) is representative of a short rod, where the rise time of the pressure disturbance is longer than the propagation time along the rod. Figure 8(d) is similar to Fig. 8(c), having the same stiffness distribution, but the mass distribution was changed to represent a solid spherical ball. The stiffness distribution in Fig. 8(d) approximates that found for the rubber ball, given that the remote element, m_1, is compressed dynamically on its flat side rather than on its curved end and is therefore similar in stiffness to its adjacent element.

VI. EXPLANATION OF MASS-SPRING CHAIN SOLUTIONS

Because only five elements were included in the model, the numerical solutions in Fig. 8 do not accurately represent the observed force waveforms, but the qualitative agreement is very good. The main features and their relevance to the experimental results are explained as follows:

A. Results for a uniform spring or a long rod [Fig. 8(a)]

The numerical solution in Fig. 8(a) shows that the force arising from a uniform mass-spring chain remains almost constant in time after an initial rise time determined by the mass and stiffness of the element in contact with the surface. If the element in contact with the surface behaves as an isolated system, then the mass m_5 would come to rest when the initial kinetic energy of m_5 is transferred to the fifth spring in the chain, in which case the compression of the fifth spring would be given by $c_5=x_5=v_1\sqrt{m_5/k_5}=0.99$ mm. Maximum compression of the fifth spring would occur at time $t=0.5\pi\sqrt{m_5/k_5}=0.50$ ms. These results are close to those found by the numerical solution for the whole chain because the compression of the fourth element in the chain is rela-

tively small when the fifth element comes to rest. Similarly, when the fourth element comes to rest, the compression of the third element is relatively small. Each element in the chain therefore behaves in a somewhat isolated manner as it compresses, and each mass element comes to rest in an ordered sequence. After coming to rest, each element is prevented from expanding by an approximately equal and opposite force exerted by the adjacent element.

The propagation of a compressional wave through the chain is in the form of a time delay between the compression of one spring and the next, and the expansion wave can also be seen clearly from the corresponding time delays for the subsequent expansion of each spring. The compression of each element in the spring is similar, with the result that each element comes to rest in turn and remains at rest until the arrival of the wave reflected from the opposite end.

The impact duration for a uniform spring or long rod impacting on a heavy block is equal to $2\sqrt{m/k}$, which is twice the transit time of a compressional wave along the spring or rod. The impact duration for the chain in Fig. 8(a) (with $m=0.1$ kg and $k=4\times10^4$ N/m) should therefore be 3.16 ms. The impact duration is found to be $\approx$3.6 ms due to the finite rise and fall time of the compression wave at the beginning and end of the impact. If the result in Fig. 8(a) is scaled by an appropriate factor, then Fig. 8(a) provides a good fit to the experimental data in Figs. 1 and 6(d).

B. Results for a medium length rod [see Fig. 8(b)]

The numerical result in Fig. 8(b) provides a good model for the experimental data in Fig. 6(c) when the time axis is scaled appropriately. If m_5 and k_5 behave as an isolated system, then m_5 would come to rest after a time $t=0.5\pi\sqrt{m_5/k_5}=0.99$ ms and the compression c_5 would be 1.98 mm. However, the fifth element contains a spring that is four times softer than the other springs, so m_5 comes to rest only when the compression c_5 is at least four times greater than c_4. Nevertheless, a compression wave can be seen propagating from the impact end of the chain to the other end, and is then reflected back as an expansion wave. The expansion wave arrives at the impact end after about 3 ms, bringing m_5 to rest and then reversing its direction of motion.

C. Results for a short rod and spherical ball [Figs. 8(c) and 8(d)]

The results in Figs. 8(c) and 8(d) can be understood by regarding each five-element chain as a single mass-spring system with stiffness $k=2\times10^4$ N/m and mass $m=0.1$ kg. The impact duration of such a system is $\pi\sqrt{m/k}=7.0$ ms and the maximum compression is $v_1\sqrt{m/k}=7.0$ mm, both values being close to those calculated for the complete five-element chain. In Figs. 8(c) and 8(d) the chain is semirigid, given that all mass elements are connected by springs that are ten times stiffer than the contact spring. In the limit where all five masses are connected by rigid rods the chain would behave as a single, rigid mass connected to a single, soft spring. The change in the mass distribution from Fig. 8(c) to Fig. 8(d) therefore makes little difference to the resulting impact force or duration. The significance of the latter result in relation to the bounce of a ball is that it is the stiffness distribution of a spherical ball that distinguishes it from a simple spring, rather than its mass distribution.

D. Impact duration

The propagation speed of the compression wave in the four cases shown in Fig. 8 is approximately the same because the stiffness of four of the five elements was held constant and because the mass of each element was the same apart from the change noted in Fig. 8(d). In all four cases c_1 began to increase about 1 ms after the initial impact, and c_1 reached its maximum value at about $t=2$ ms. The expansion wave returned to the impact end of the chain at about $t=3$ ms, causing the whole chain to bounce off the surface at $t=3.6$ ms in Fig. 8(a). The impact duration was longer in the other three cases due to the slower compression and the slower expansion at the impact end of the chain. As a result the compressional wave in Figs. 8(c) and 8(d) made about four transits up and down the chain during the impact, experiencing only partial reflection off each end of the chain.

The parameters in Figs. 8(b)–8(d) are approximately the same as those for the rubber ball described in Sec. III, resulting in an impact duration and maximum compression similar to those shown in Fig. 3. It can be deduced that the compressional wave in the rubber ball made three or four transits across the ball during the bounce. In Fig. 3 the ball was dropped from a height of 50 cm and the impact duration was 5.9 ms. When dropped from a height of 1 mm the impact time of the rubber ball extended to 12 ms due to the decrease in stiffness at the impact end of the ball, in which case the compressional wave in the ball made about 8 transits across the ball during the impact. A more realistic model of the ball would therefore require a nonlinear spring at the impact end, but there would be no need to include more than two elements in the mass-spring chain.

E. Coefficient of restitution

An interesting observation arising from Fig. 8(d) is that 94% of the elastic energy stored in the chain is stored in the element in contact with the surface, a result that is easily verified by summing $0.5k_ic_i^2$ over the five elements, the total being equal to the incident kinetic energy of the ball, 0.49 J. Consequently, most of the energy lost in the rubber ball is likely to be dissipated in the contact region of the ball. A similar result cannot be assumed for all balls, especially if the coefficient of restitution is relatively high, as it is for steel balls. Some of the elastic energy stored in each chain shown in Fig. 8 is dissipated as vibrational energy throughout the chain. No specific energy loss dissipation mechanism was included in the model, but the coefficient of restitution for each chain varied from 0.975 in Figs. 8(a) and 8(b) to 0.996 in Figs. 8(c) and 8(d), indicating that a small amount of vibrational energy was retained in each chain after it bounced off the surface. The coefficient of restitution was calculated as the ratio of the center of mass speed after the collision to that before the collision.

VII. COLLIDING BALLS AND COLLIDING SPRINGS

If a light steel ball collides head-on with a heavy steel ball, and if the heavy ball is initially at rest, then the light ball will bounce backward and both balls will move off in opposite directions with very little loss in kinetic energy. Auerbach[6] analyzed an analogous problem involving the longitudinal collision of two steel rods. He found that the results were dramatically different to those observed with steel balls. If a

short rod of length L_1 collides with a stationary rod of length $L_2 > L_1$, then the short rod comes to rest regardless of the mass or length of the longer rod. Because momentum is conserved, the long rod moves off with a fraction L_1/L_2 of the initial energy. The coefficient of restitution for the collision is given by L_1/L_2 when $L_2 > L_1$. Auerbach[6] explained the loss of energy in terms of the vibrational energy stored in the longer rod after the collision, concluding that the conservation of kinetic energy in a collision between two steel balls of different mass is mysterious. Bayman[4] provided an analogous solution for the end-on collision between two springs and also had difficulty explaining why kinetic energy should be conserved in a collision between two steel balls of different diameters.

The collision between two uniform springs can be analyzed by a simple extension of the model described in Sec. V by replacing the heavy block by an initially stationary, five-element spring. The numerical solution for a collision between spring A (mass $m=0.145$ kg, length $L=0.18$ m, and stiffness $k=9100$ N/m) and the block resulted in an impact duration of 8.7 ms with a coefficient of restitution of 0.97. When colliding with an identical spring, the numerical solution resulted in an impact duration of 9.0 ms and a coefficient of restitution of 0.92. For a collision with a five-element spring of twice the mass and half the stiffness (to simulate a spring with $L_2/L_1=2$), the numerical solution resulted in an impact of duration 9.0 ms and a coefficient of restitution of 0.54. In both cases the velocity of the incident spring was negligible after the collision. Apart from small errors introduced by including only five elements to model each spring, the numerical results are consistent with the analytical solutions in Refs. 6 and 4.

The collision between two balls can also be modeled in the same manner as the collision between two five-element springs. The total mass of each ball can be taken to be proportional to its radius cubed and the stiffness of each ball can taken to be proportional to its radius.[17] A simpler approach would be to model each ball as single element mass and spring because that is the result found for the five element chain in Fig. 8(d). This approach can be justified on the basis that a negligible fraction of the stored elastic energy in a bouncing ball is retained as vibrational energy even when the compression wave in the ball propagates across the ball a noninteger number of times during the bounce period. When a bouncing or colliding ball compresses, it does so by storing most of its elastic energy in the contact region and very little energy propagates away from the contact region as a compression wave. As shown in Figs. 8(b)–8(d), the amplitude of the compression wave is much smaller than the compression of the contact region, and the energy content in the compression wave is also very small. A similar result would be obtained by striking a steel ball or a steel rod with a rubber hammer rather than a steel hammer because the impact duration would be too long to excite any high frequency mode in the ball or the rod. The frequency spectrum of an impact of duration T extends to about $1.5/T$ but no longer than that. Consequently, when one ball collides with another, only a small fraction of the initial energy is converted to acoustic waves in the two balls, leaving the possibility that kinetic energy will be conserved if both balls are highly elastic.

Our interpretation of the collision events is consistent with previous calculations regarding the generation of acoustic waves when an elastic sphere collides with a heavy, elastic block. It has been shown theoretically by several authors[18,19] that only a small fraction of the initial kinetic energy is transferred to the block as a result of wave generation in the block. For example, when a small ball bearing is dropped on a thick sheet of glass, the coefficient of restitution is about 0.985, a result that is consistent with the generation of acoustic waves in the glass.[19]

VIII. CONCLUSIONS

The bounce properties of various balls, springs, and rods were measured and found to be qualitatively consistent with a simple mass-spring chain model in all cases. The impact duration of a spring (or a long rod) bouncing off a heavy, rigid surface or off another spring (or rod) depends on the propagation time of a compression wave from the impact point to the other end and back again. The impact force on the spring or the rod remains approximately constant in time.

The impact duration of a medium length rod is longer than the return trip of a compression wave along the rod because the pressure disturbance at the impact end has a rise and a fall time that is comparable with the transit time of the compression wave. The impact duration of a short rod or a spherical ball or a long rod with a soft tip is determined by the mass of the rod or ball and by the stiffness of the impact region. The impact duration, T, is much longer than the transit time τ of a compression wave along the rod or across the ball. Each object behaves like a single mass at the end of a spring, and the impact force varies in a sinusoidal manner for one half cycle of oscillation. The vibrational energy remaining after the collision is generally negligible because the impact duration is too long to excite any high frequency modes in the object. The frequency spectrum of the impact force waveform extends from zero to about $1.5/T$ and does not extend to $1/\tau$, and hence even the fundamental vibration mode is suppressed. Consequently, steel balls of unequal diameter conserve kinetic energy when they collide, but springs or long rods of unequal length do not.

[a]Electronic mail: cross@physics.usyd.edu.au

[1] J. M. Aguirregabiria, A. Hernandez, and R. Rivas, "Falling elastic bars and springs," Am. J. Phys. **75**, 583–587 (2007).
[2] M. G. Calkin, "Motion of a falling spring," Am. J. Phys. **61**, 261–264 (1993).
[3] A. P. French, *Vibrations and Waves* (Norton, New York, 1971).
[4] B. F. Bayman, "Model of the behavior of solid objects during collision," Am. J. Phys. **44**, 671–676 (1976).
[5] W. G. Britton, J. J. Fendley, and M. E. Michael, "Longitudinal impact of rods: A continuing experiment," Am. J. Phys. **46**, 1124–1130 (1978).
[6] D. Auerbach, "Colliding rods: Dynamics and relevance to colliding balls," Am. J. Phys. **62**, 522–525 (1994).
[7] F. M. F. Mascarenhaus, C. M. Spillmann, J. F. Lindner, and D. T. Jacobs, "Hearing the shape of a rod by the sound of its collision," Am. J. Phys. **66**, 692–697 (1998).
[8] P. Roura, "Collision duration in the elastic regime," Phys. Teach. **35**, 435–436 (1997).
[9] P. Roura, "Collisions between rods: A visual analysis," Phys. Teach. **41**, 32–35 (2003).
[10] F. Herrmann and P. Schmalzle, "Simple explanation of a well-known collision experiment," Am. J. Phys. **49**, 761–764 (1981).
[11] F. Herrman and M. Seitz, "How does the ball-chain work?," Am. J. Phys. **50**, 977–981 (1982).
[12] R. Hessel, A. C. Perinotto, R. A. M. Alfaro, and A. A. Freschi, "Force-versus-time curves during collisions between two identical steel balls," Am. J. Phys. **74**, 176–179 (2006).
[13] R. Cross, "The bounce of a ball," Am. J. Phys. **67**, 222–227 (1999).
[14] B. Leroy, "Collision between two balls accompanied by deformation: A

qualitative approach to Hertz's theory," Am. J. Phys. **53**, 346–349 (1985).
[15]E. N. Martinez, "Effective mass of a classical linear chain," Am. J. Phys. **61**, 1102–1110 (1993).
[16]M. Reinsch, "Dispersion-free linear chains," Am. J. Phys. **62**, 271–278 (1994).
[17]R. Cross, "Vertical bounce of two vertically aligned balls," Am. J. Phys. **75**, 1009–1016 (2007).
[18]I. M. Hutchings, "Energy absorbed by elastic waves during plastic impact," J. Phys. D **12**, 1819–1824 (1979).
[19]J. Reed, "Energy losses due to elastic wave propagation during an elastic impact," J. Phys. D **18**, 2329–2337 (1985).

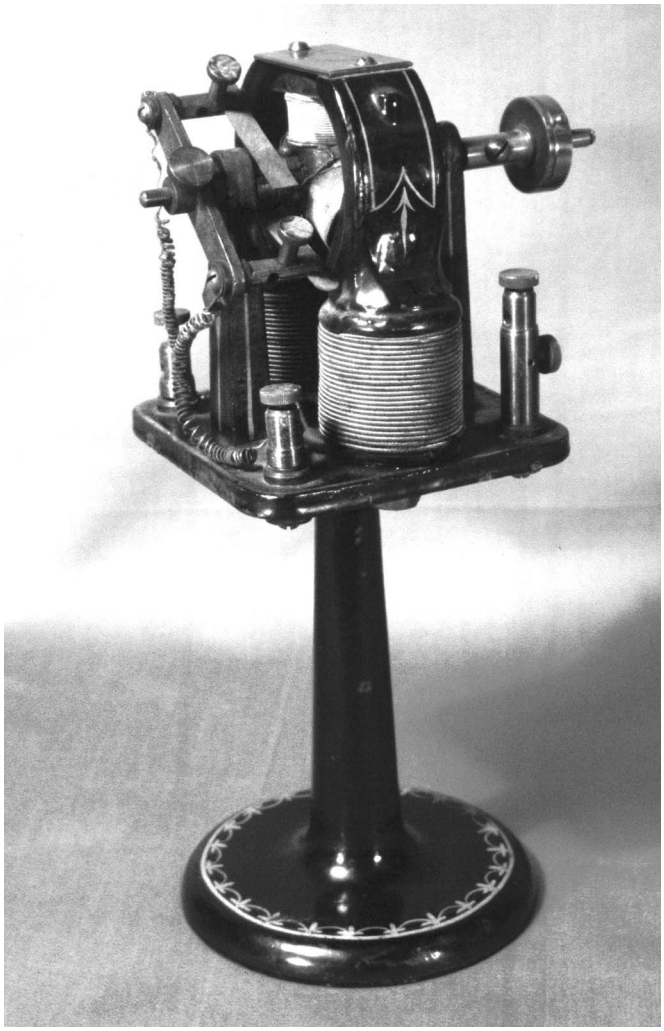

Geissler Tube Rotator. This motor was designed to rotate elaborately-shaped discharge tubes in a demonstration that passed the line between physics and art. It is listed in the 1916 catalogue of the L.E. Knott Apparatus Co. of Boston as being used "for rotating Geissler Tubes to increase the spectacular effect. Our Rotator consists of a practical motor (not a toy) constructed after designs of the expensive commercial types. It is ... provided with appropriate binding posts, one pair for battery or other current and one pair for induction coil or Influence Machine. The Geissler tube is attached to the holder, which may be firmly fixed to the spindle of the rotator." For battery power it cost $12.00, and models for 110 volts D.C. and 110 volts A.C. were $13.25. The motor is at St. Mary's College in Notre Dame, Indiana. (Photograph and Notes by Thomas B. Greenslade, Jr., Kenyon College)